THE DIFFUSE PHASE TRANSITION OF Ti-RICH $(Ba_{0.75}Sr_{0.25})$ $Ti_{1+\delta}O_{3+2\delta}$ DIELECTRIC CERAMICS

PREHOD DIFUZIVNE FAZE V DIELEKTRIČNE KERAMIKE, BOGATE S Ti $((Ba_{0.75}Sr_{0.25})$ $Ti_{1+\delta}O_{3+2\delta})$

Chen Zhang*, Xin Zhong, Fang-Xu Chen, Zhu-Ming Tang

Jiangsu University of Science and Technology, Department of Materials Science and Engineering, No. 2 Mengxi Road,
Zhenjiang 212004, China

The microstructures, dielectric properties and phase-transition behavior of Ti-rich barium-strontium-titanate-based ceramics synthesized by the solid-state method were investigated with a non-stoichiometric level by SEM, XRD and an LCR measuring system. It was found that all the $(Ba_{0.75}Sr_{0.25})Ti_{1+\delta}O_{3+2\delta}$ ceramics (δ = 0.005, 0.01, 0.015, 0.02) are single-phase solid solutions with a typical tetragonal perovskite structure. With an increasing δ value, the average grain size of the $(Ba_{0.75}Sr_{0.25})Ti_{1+\delta}O_{3+2\delta}$ ceramics increases. The strengthened spontaneous polarization resulting from the unit-cell deformation is responsible for the increase of the transition temperature T_m as δ increases. Also, the dielectric parameters ε_{rRT} and ε_m increase with an increasing non-stoichiometric level. The low-temperature ($T \leq T_m$) frequency dispersion of the relative dielectric constant can be found and the diffuse phase-transition behavior is suppressed with an increasing δ value in the $(Ba_{0.75}Sr_{0.25})Ti_{1+\delta}O_{3+2\delta}$ ceramics.

Keywords: barium strontium titanate, dielectrics, ceramics, phase transition

Avtorji so analizirali mikrostrukture, dielektrične lastnosti in fazne prehode barij-stroncij titanatne kermamike bogate s Ti, ki so jo sintetizirali z metodo sintranja v trdni fazi. Analize na nestehiometričnem nivoju so izvajali s pomočjo SEM, XRD in LCR preiskovalnih sistemov. Ugotovili so da vsebuje $(Ba_{0.75}Sr_{0.25})Ti_{1+\delta}O_{3+2\delta}$ keramika (pri δ = 0,005, 0,01, 0,015 ali 0,02) enofazno trdno raztopino s tipično tetragonalno peroviskitno strukturo. Z naraščajočo vrednostjo d narašča povprečna velikost kristalnih zrn $(Ba_{0.75}Sr_{0.25})Ti_{1+\delta}O_{3+2\delta}$ keramike. Ojačana spontana polarizacija je posledica deformacije enovite celice, kar povzroči z naraščajočim d tudi naraščanje temperature prehoda T_m. Prav tako s povečevanjem nestehiometrije naraščata dielektrična parametra ε_{rRT} in ε_m. Ugotovili so tudi, da ima z naraščajočo vrednostjo d $(Ba_{0.75}Sr_{0.25})Ti_{1+\delta}O_{3+2\delta}$ keramika nizko disperzijo temperaturne frekvence ($T = T_m$) relativne dielektrične konstante in zatrt prehod difuzivne faze.

Ključne besede: barij stroncijev titanat, dielektriki, keramika, fazni prehodi

1 INTRODUCTION

Ferroelectric barium titanate ($BaTiO_3$, BT) possesses a typical perovskite structure ABO_3, which is used in many electronic devices, including high-permittivity multilayer ceramic capacitors (MLCC's).[1] The interest in BT stems from the high relative permittivity 10,000–12,000, observed at the ferro- to para-electric phase-transition temperature (about 130 ºC), also known as the Curie temperature T_c.[2] Above T_c, in the paraelectric state, the temperature dependence of the dielectric constant follows the Curie-Weiss law and around T_c, a sharp Curie peak can always be found.

To meet the tolerances of the percentage change of capacitance ΔC over a certain temperature range ΔT for the different specifications of MLCCs, various dopants are often applied in BT dielectric ceramics.[3–5] The majority of dopants added into BT cause a drop of T_c, and some of them succeed in inducing the diffuse phase transition. For example, the substitution of Zr^{4+} with isovalent Ti^{4+} results in a solid solution from BT to $Ba(Ti_{1-x}Zr_x)O_3$ (BZT) and causes typical relaxor ferroelectric behavior characterized by the frequency dispersion of the relative permittivity maximum as well as a diffuse phase transition as x approaches 0.3.[6,7] However, some of the dopants fail to modify the temperature stability of the capacitance, especially around the T_c. For instance, the solid solution $(Ba_{1-x}Sr_x)TiO_3$ (BST) resulting from the substitution of Sr^{2+} with isovalent Ba^{2+} in BT still has a sharp Curie peak, even when x equals 0.4.[8]

For practical capacitor applications, a further modification in BST ceramics is inevitable. Three common methods are employed: the addition of isovalent or aliovalent dopants such as Mg,[9] Na,[10] etc.; process controlling especially the calcination/sintering progress;[11,12] and the usage of functionally graded materials (FGMs).[8] Among the dopants, rare-earth elements (e.g., La^{3+}, Dy^{3+}, Sm^{3+}) are found to be effective in controlling the temperature dependency of the dielectric properties in stoichiometric BST ceramics.[13–15] The diffused ferro-electric-paraelectric phase transition accompanied by the comprehensive properties can be obtained in Ho_2O_3 highly doped $(Ba_{0.75}Sr_{0.25})TiO_3$ ceramics according to our previous study.[16] The high unchanged dielectric constant with a slight decrease of loss tangent has been found in

*Corresponding author's e-mail:
czhang1981@hotmail.com (Chen Zhang)

Ba-excessive $Ba_{0.71}Sr_{0.29}TiO_3$ ceramics[17] and adding deficient TiO_2 could bring about a diffuse phase transition in BST ceramics,[18] which provides us with the possibility to obtain fine dielectrics for ceramic capacitors by controlling the mole ratio of A-site ion to B-site ion ($n_A:n_B$) in BST ceramics. Furthermore, the dielectric temperature stability of the BST ceramics can be somehow improved by applying excessive TiO_2.[19]

Previous findings sparked our interest in findind out how the Ti-rich level influencing the dielectric properties and phase-transition behavior in non-stoichiometric BST ceramics modified with Ho_2O_3. Therefore, in this article we report a systematic study of the microstructure, dielectric properties and phase transition of non-stoichiometric $(Ba_{0.75}Sr_{0.25})Ti_{1+\delta}O_{3+2\delta}$ (δ = 0–0.02) based ceramics [$n_A:n_B$ =1:(1+δ)≤1].

2 EXPERIMENTAL PART

The chemical compositions of the Ti-rich BST-based ceramics were given by the formula $(Ba_{0.75}Sr_{0.25})$ $Ti_{1+\delta}O_{3+2\delta}$ + 3 at.% Ho_2O_3 (δ = 0, 0.005, 0.01, 0.015, 0.02) and symbolized as R0, R1, R2, R3, R4. High-purity $BaCO_3$ (>99.0 %), $SrCO_3$ (>99.0 %) and TiO_2 (>98.0 %) powders used as starting raw materials were weighed, ball-milled, dried and calcined at 1080 °C for 2 h. The calcined powders were mixed with Ho_2O_3 (>99.0 %), reground, dried and added with 5 % (w/%) polyvinyl alcohol (PVA) as a binder for granulation. The mixture was sieved through a 60-mesh screen and then pressed into pellets. Sintering was conducted in air at 1350–1480 °C for 1–6 h. For dielectric the measurements, both the flat surfaces of the specimens were coated with BQ-5311 silver paste after ultrasonic bath cleaning and then fired at 800 °C for 10 min.

The crystal structures of the specimens were confirmed by X-ray diffraction analysis (XRD, Rigaku D/max 2500v/pc) with Cu-K_α radiation. The surface morphologies of the as-sintered specimens were observed using the SEM (JSM-6480 ESEM). The temperature dependence of the dielectric constant and loss tangent was measured at 1 kHz, 10 kHz, 100 kHz and 500 kHz from –185 °C to 250 °C with a TZDM-200-300 automatic LCR measuring system. The percentage of permittivity variation at 1 kHz ($\Delta\varepsilon_r/\varepsilon_r$) from –30 °C to 85 °C used for accessing the temperature stability of the relative dielectric constant is determined using the following Equation:

$$\frac{\Delta\varepsilon_r}{\varepsilon_r} = \frac{\varepsilon_{rt} - \varepsilon_{rRT}}{\varepsilon_{rRT}} \times 100\% \qquad (1)$$

where ε_{rRT} is the relative dielectric constant at room temperature; ε_{rt} is the relative dielectric constant at any other temperature. All the above microstructure analyses and dielectric measurements were conducted using the samples sintered at 1450 °C for 2 h.

3 RESULTS AND DISCUSSION

The X-ray diffraction patterns of the as sintered $(Ba_{0.75}Sr_{0.25})Ti_{1+\delta}O_{3+2\delta}$ bulk ceramics are shown in **Figure 1**. It appears that the stoichiometric ceramic $(Ba_{0.75}Sr_{0.25})TiO_3$ and the non-stoichiometric $(Ba_{0.75}Sr_{0.25})$ $Ti_{1+\delta}O_{3+2\delta}$ ceramics (δ = 0.005, 0.01, 0.015, 0.02) are single-phase solid solutions with a typical perovskite structure. No obvious secondary phase is detected, even for the $(Ba_{0.75}Sr_{0.25})Ti_{1.02}O_{3.04}$ ceramics based on the X-ray diffraction patterns. According to the magnified view of the diffraction peaks presented in **Figures 1b** and **1c**, the (002)/(200) and (202)/(220) diffraction peaks
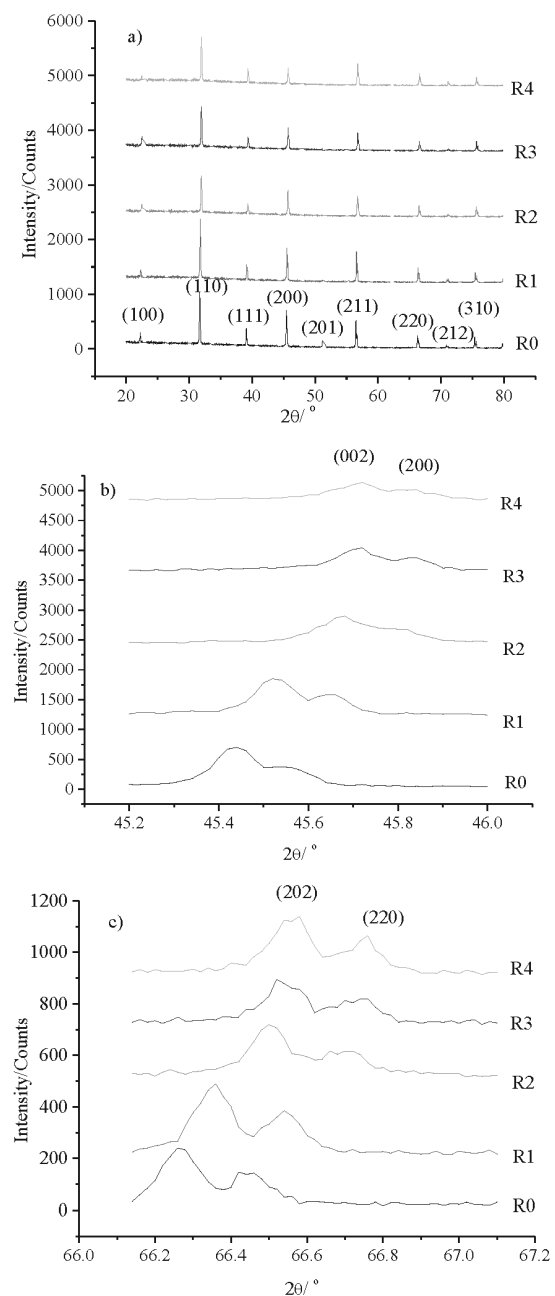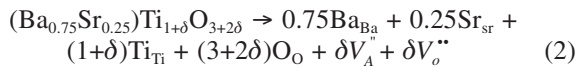

Figure 1: XRD patterns for $(Ba_{0.75}Sr_{0.25})Ti_{1+\delta}O_{3+2\delta}$ ceramics

can be seen in all the (Ba$_{0.75}$Sr$_{0.25}$)Ti$_{1+\delta}$O$_{3+2\delta}$ ceramics, indicating that the studied ceramics possess tetragonal perovskite structure (space group P4mm).

Also, a slight shift of the diffraction peaks to higher two-theta values with the increasing δ value is observed, which indicates that the unit-cell volumes of the (Ba$_{0.75}$Sr$_{0.25}$)Ti$_{1+\delta}$O$_{3+2\delta}$ ceramics decrease as the non-stoichiometric level of the Ti ions present in the ABO$_3$ perovskite structure increases. Similar phenomena have been previously reported in Ca-substituted BST ceramics[20] and in our previous work for Ti deficient (Ba$_{0.75}$Sr$_{0.25}$)Ti$_{1-\delta}$O$_{3-2\delta}$ ceramics.[21]

Initially, the A-site vacancies $V_A^{''}$ and oxygen vacancies $V_o^{\bullet\bullet}$ remain in the un-doped (Ba$_{0.75}$Sr$_{0.25}$)Ti$_{1+\delta}$O$_{3+2\delta}$ calcined powders according to the following point-defect reaction equation:

$$(Ba_{0.75}Sr_{0.25})Ti_{1+\delta}O_{3+2\delta} \rightarrow 0.75Ba_{Ba} + 0.25Sr_{sr} + (1+\delta)Ti_{Ti} + (3+2\delta)O_O + \delta V_A^{''} + \delta V_o^{\bullet\bullet} \qquad (2)$$

After Ho$_2$O$_3$ doping, the A-site vacancies $V_A^{''}$ are partially filled up by Ho^{3+} ions forming the point defects Ho$_A^{\bullet}$ and the leftover A-site vacancies $V_A^{''}$ taking the negative charge remain there to compensate the positive charge of Ho$_A^{\bullet}$. After that, the Ho^{3+} ions begin to substitute the host ions (including both the A-site ion and B-site ion) because the concentration of Ho^{3+} doping ions (6 at.%) is much more than that of the A-site

vacancies (less than or equal to 2 $a/\%$). And the other two point defect reactions happen:

$$Ho_2O_3 \rightarrow 2Ho_A^{\bullet} + V_A^{''} + 3O_O \qquad (3)$$

$$Ho_2O_3 \rightarrow 2Ho_{Ti}^{'} + V_o^{\bullet\bullet} + 3O_O \qquad (4)$$
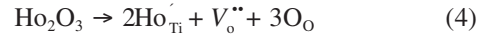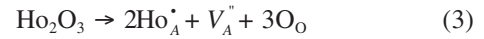
Therefore, there are totally four kinds of point defects Ho$_{Ti}^{'}$, Ho$_A^{\bullet}$, $V_A^{''}$ and $V_o^{\bullet\bullet}$ in the Ho$_2$O$_3$ doped (Ba$_{0.75}$Sr$_{0.25}$)Ti$_{1+\delta}$O$_{3+2\delta}$ ceramics. With the increase of δ, the amount of Ho^{3+} ion occupying the A-site increases, while that in the B-site decreases due to the fixed concentration of Ho^{3+} ions. The radii of the host Ba^{2+} and Sr^{2+} ions are 0.161 nm (in 12 coordination) and 0.144 nm (in 12 coordination), respectively, while the radius of the host Ti^{4+} ion is 0.061 nm (in 6 coordination). The Ho^{3+} doping ion with a moderate radius of 0.0901 nm can cause the shrinkage of the unit cell by entering the A-site or the unit-cell expansion by getting into the B-site due to the radius difference between the Ho^{3+} ion and the host ion. Apparently, the obtained shrinkage of the unit-cell volume with the increase of δ in (Ba$_{0.75}$Sr$_{0.25}$)Ti$_{1+\delta}$O$_{3+2\delta}$ ceramics is exactly attributed to the above-mentioned difference of the Ho^{3+} distribution in the host lattice site when increasing δ.

Figure 2 shows the surface morphologies of the as-sintered (Ba$_{0.75}$Sr$_{0.25}$)Ti$_{1+\delta}$O$_{3+2\delta}$ ceramics. All the (Ba$_{0.75}$Sr$_{0.25}$)Ti$_{1+\delta}$O$_{3+2\delta}$ samples possess dense microstructures and a fine grain size distribution can be found in
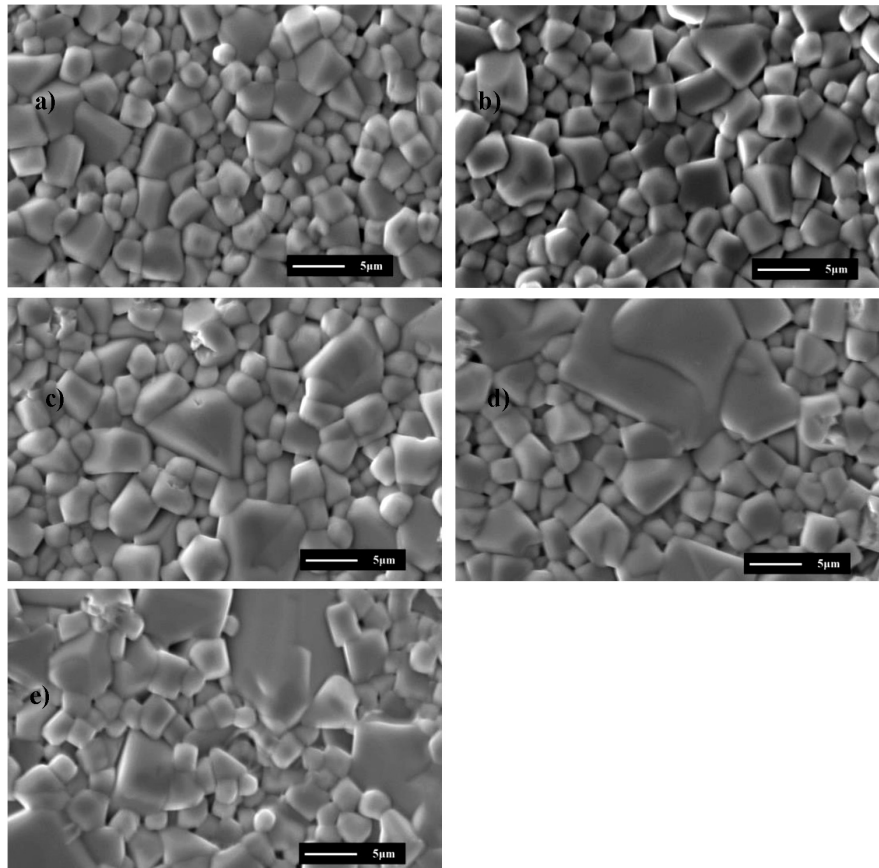
Figure 2: SEM micrographs of (Ba$_{0.75}$Sr$_{0.25}$)Ti$_{1+\delta}$O$_{3+2\delta}$ ceramics: a) $\delta = 0$, b) $\delta = 0.005$, c) $\delta = 0.01$, d) $\delta = 0.015$, e) $\delta = 0.02$
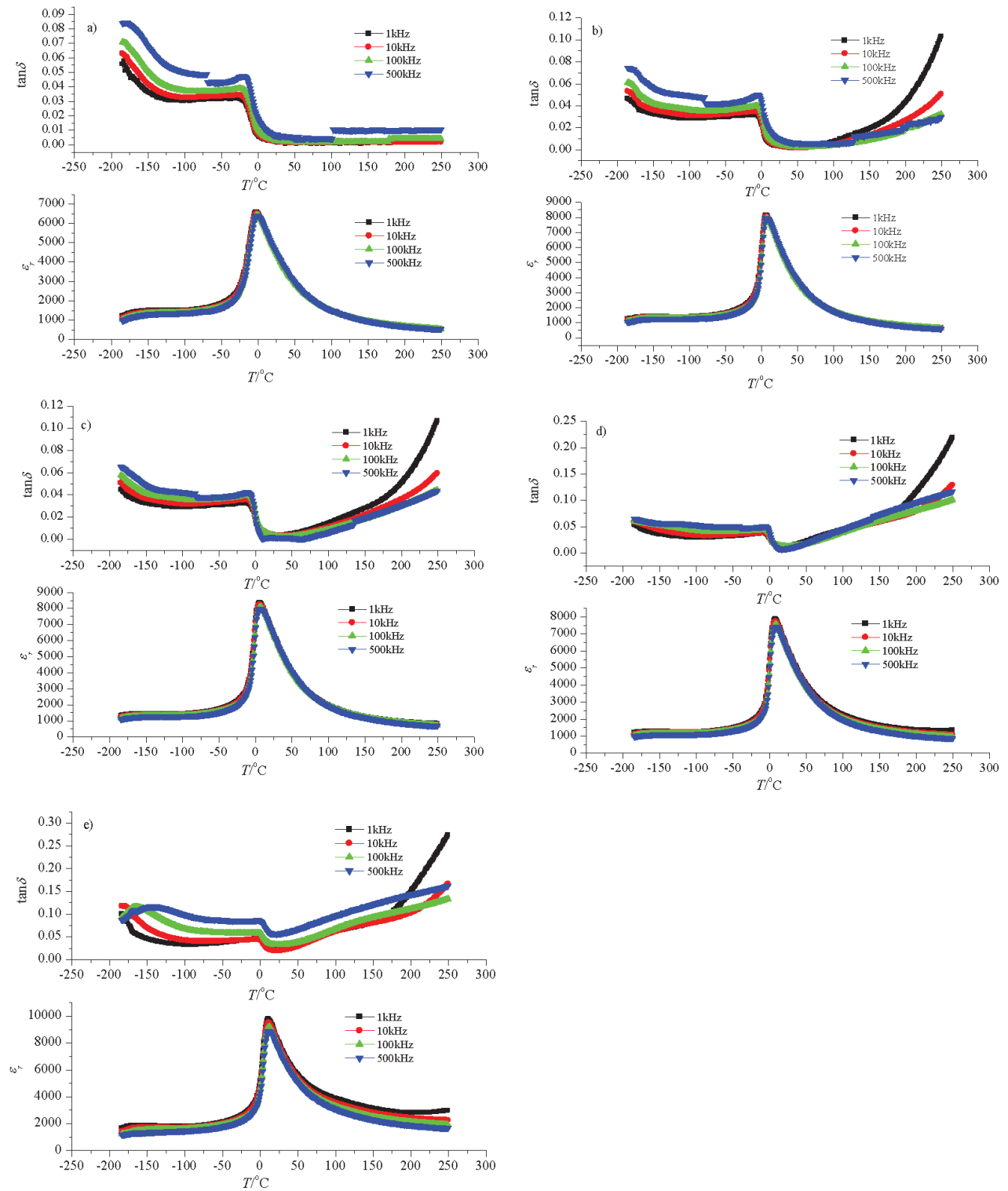
Figure 3: Temperature dependence of the relative dielectric constant and loss tangent for $(Ba_{0.75}Sr_{0.25})Ti_{1+\delta}O_{3+2\delta}$ ceramics at different frequencies: a) $\delta = 0$, b) $\delta = 0.005$, c) $\delta = 0.01$, d) $\delta = 0.015$, e) $\delta = 0.02$

ceramics with a small δ value. However, with the increase of δ, the abnormal grain growth becomes distinct, as shown in **Figures 2c, 2d** and **2e**. The average grain size of the (Ba$_{0.75}$Sr$_{0.25}$)Ti$_{1+\delta}$O$_{3+2\delta}$ ceramics analyzed using the Nano Measurer software is collected in **Table 1**. It is obvious that the average grain size of the (Ba$_{0.75}$Sr$_{0.25}$)Ti$_{1+\delta}$O$_{3+2\delta}$ ceramics increases with the increasing δ value.

Table 1: Average grain size of (Ba$_{0.75}$Sr$_{0.25}$)Ti$_{1+\delta}$O$_{3+2\delta}$ ceramics

Sample No.	R0	R1	R2	R3	R4
Grain size(μm)	2.1	2.6	2.8	2.9	3.1

Figure 3 shows the temperature dependence of the relative dielectric constant and dielectric loss for the (Ba$_{0.75}$Sr$_{0.25}$)Ti$_{1+\delta}$O$_{3+2\delta}$ ceramics at 1 kHz, 10 kHz, 100 kHz and 500 kHz. The dielectric constant peaks corresponding to the ferroelectric-paraelectric phase transition can be observed for all the (Ba$_{0.75}$Sr$_{0.25}$) Ti$_{1+\delta}$O$_{3+2\delta}$ ceramics. The relative dielectric constant at room temperature (25 °C) ε_{rRT}, the loss tangent at room temperature (25 °C) tan δ_{RT}, the maximum of dielectric permittivity ε_m at 1 kHz and the temperature corresponding to this permittivity maximum T_m are collected in **Table 2**. The ε_{rRT}, tan δ_{RT} and ε_m increase with the increasing δ value, in general. The (Ba$_{0.75}$Sr$_{0.25}$)Ti$_{1+\delta}$O$_{3+2\delta}$ ceramics with low δ value, such as R1 and R2, possess a high relative dielectric constant (>6000) and a low dielectric loss (<0.004) at room temperature. With the increase of δ value, the T_m increase from –1 °C for R0 to 6 °C for R2 and then to 12 °C for R4. The rise of T_m is also found in samarium-doped Ba$_{0.68}$Sr$_{0.32}$TiO$_3$ ceramics.[15] The charged vacancies, such as A-site vacancies $V_A^{''}$ and oxygen vacancies $V_o^{\cdot\cdot}$ in (Ba$_{0.75}$Sr$_{0.25}$) Ti$_{1+\delta}$O$_{3+2\delta}$ ceramics, as mentioned previously, give rise to the distortion of the ABO$_3$ perovskite unit cells and thus a stronger deviation of the B-site ion from the center of the oxygen octahedron. It is exactly this stronger deviation that explains the enhancement of the spontaneous polarization, in other words, the increased tetragonality in tetragonal BST perovskites. Therefore, the increase of T_m with the increasing δ is observed. The increase of ε_{rRT} and ε_m with increasing δ is also attributed to the strengthened spontaneous polarization. It has been reported that the smaller grains in ferroelectric ceramics inhibit the formation of large ferroelectric domains and thus reduce the effective contribution to the total polarization.[22] Furthermore, the (Ba$_{0.75}$Sr$_{0.25}$)Ti$_{1+\delta}$O$_{3+2\delta}$ ferroelectric ceramics with a smaller grain size contain more non-ferroelectric grain boundaries but relatively fewer ferroelectric grains than those with a larger grain size. Therefore, the increased average grain size gives another reason for the increase of ε_{rRT} and ε_m with increasing δ. The $\Delta\varepsilon_r/\varepsilon_r$ at 1 kHz from –30 °C to 85 °C for the (Ba$_{0.75}$Sr$_{0.25}$)Ti$_{1+\delta}$O$_{3+2\delta}$ ceramics is shown in **Table 2**. The $\Delta\varepsilon_r/\varepsilon_r$ of R4 sample (+20.0 % − –68.7 %) satisfies the Y5V standard ($\Delta\varepsilon_r/\varepsilon_r \leq$ +22 % to –82 % from –30 °C to

85 °C) according to the ceramic capacitor classification of the Electronic Industries Association (EIA).[18,23]

The low temperature ($T \leq T_m$) frequency dispersion of the relative dielectric constant can be found in (Ba$_{0.75}$Sr$_{0.25}$)Ti$_{1+\delta}$O$_{3+2\delta}$ ceramics. The dielectric loss of (Ba$_{0.75}$Sr$_{0.25}$)Ti$_{1+\delta}$O$_{3+2\delta}$ ceramics shows the strong frequency dependence across the whole temperature range.

Table 2: Dielectric parameters for (Ba$_{0.75}$Sr$_{0.25}$)Ti$_{1+\delta}$O$_{3+2\delta}$ ceramics at 1 kHz

Sample No.	δ	ε_{rRT}	tan δ_{RT}	ε_m	$\Delta\varepsilon_r/\varepsilon_r$ (%)
R0	0	4469	0.0017	6565	+46.9– –60.8
R1	0.005	6159	0.0022	8123	+31.9– –67.1
R2	0.01	6478	0.0039	8330	+28.6– –66.6
R3	0.015	6172	0.0122	7842	+27.1– –70.5
R4	0.02	8119	0.0220	9742	+20.0– –68.7

The diffuse phase transition is always characterized by a deviation from the Curie-Weiss law in the vicinity of the Curie temperature (T_c). It is known that the dielectric permittivity of a normal ferroelectric above the Curie temperature follows the Curie-Weiss law described by the following Equation (5):

$$\frac{1}{\varepsilon_r} = \frac{T - T_0}{C} \qquad (5)$$

where T_0 is the Curie-Weiss temperature and C is the Curie-Weiss constant. **Figure 4** shows the inverse of the relative dielectric constant for (Ba$_{0.75}$Sr$_{0.25}$)Ti$_{1+\delta}$O$_{3+2\delta}$ ceramics as a function of temperature at 1 kHz. The plots (for the $T > T_m$ part) are fitted linearly according to Equation (5) and the Curie-Weiss temperature T_0 obtained from the fittings is listed in **Table 3**.

Obviously, the dielectric behavior of the (Ba$_{0.75}$Sr$_{0.25}$) Ti$_{1+\delta}$O$_{3+2\delta}$ ceramics with a low δ value shows a deviation from the Curie-Weiss law at temperatures above the T_m.
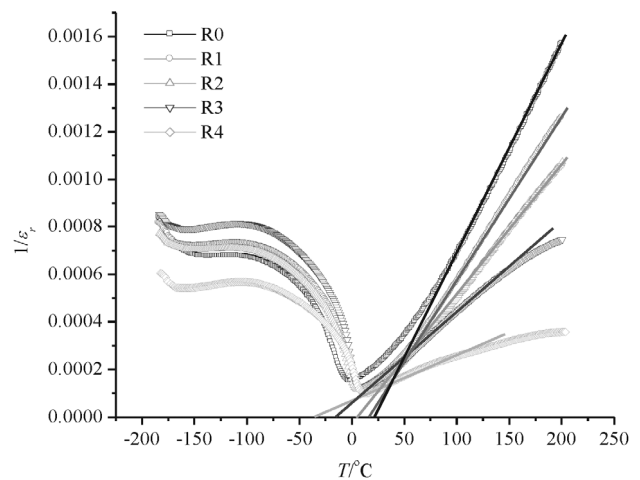
Figure 4: Temperature dependence of the inverse relative dielectric constant for (Ba$_{0.75}$Sr$_{0.25}$)Ti$_{1+\delta}$O$_{3+2\delta}$ ceramics at 1 kHz (The symbols: experimental data; the solid line: fitting to the Curie-Weiss law.)

Then the parameter ΔT_m, often used to characterize the degree of the deviation from the Curie-Weiss law and defined as follows, is calculated (**Table 3**):

$$\Delta T_m = T_{cw} - T_m \qquad (6)$$

where T_{cw} denotes the temperature from which the dielectric permittivity starts to deviate from the Curie-Weiss law and T_m represents the temperature of the dielectric constant maximum. With the increase of the δ value, ΔT_m decreases from 79 °C (for R0 sample) to 1 °C (for R4 samples), which indicates that the diffuse transition behavior is suppressed with an increasing δ value and the diffuse phase-transition behavior of (Ba$_{0.75}$Sr$_{0.25}$)Ti$_{1+\delta}$O$_{3+2\delta}$ ceramics even vanishes at $\delta = 0.02$.

Table 3: Temperature parameters for (Ba$_{0.75}$Sr$_{0.25}$)Ti$_{1+\delta}$O$_{3+2\delta}$ ceramics at 1 kHz

Sample No.	δ	T_0 (°C)	T_{cw} (°C)	T_m (°C)	ΔT_m (°C)
R0	0	21	78	−1	79
R1	0.005	16	59	7	52
R2	0.01	4	37	6	31
R3	0.015	−16	18	8	10
R4	0.02	−37	11	12	1

A modified Curie-Weiss law has been proposed to describe the diffuseness of the ferroelectric phase transition:

$$\frac{1}{\varepsilon_r} - \frac{1}{\varepsilon_m} = \frac{(T-T_m)^\gamma}{C} \qquad (7)$$

where γ and C' are assumed to be constant. The parameter γ reveals the characteristic of the phase transition: for $\gamma = 1$, a normal Curie-Weiss law is obtained; for $\gamma = 2$, a complete diffuse phase transition is described. The parameters γ can be obtained by a linear fitting of the data through $\ln(1/\varepsilon_r - 1/\varepsilon_m) \sim \ln(T-T_m)$. The plots of
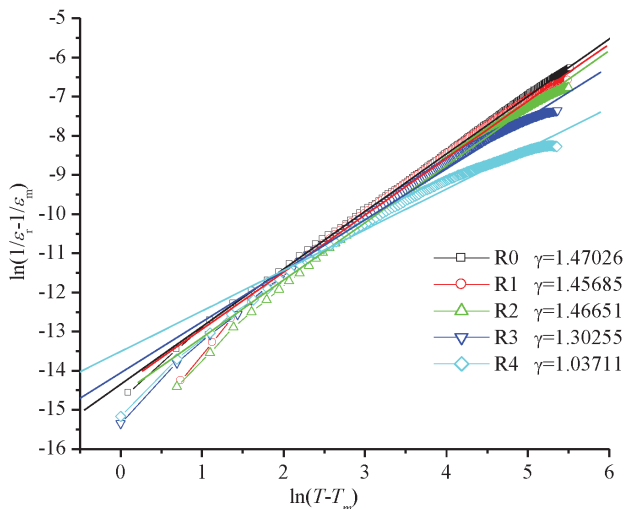
$\ln(1/\varepsilon_r - 1/\varepsilon_m)$ as a function of $\ln(T-T_m)$ for (Ba$_{0.75}$Sr$_{0.25}$)Ti$_{1+\delta}$O$_{3+2\delta}$ samples are shown in **Figure 5**. The $\gamma =$ 1.47026, 1.46651, 1.30255 and 1.03711, respectively, for R0, R2, R3 and R4 ceramics. The γ value decreases as the δ increases, clearly implying that the (Ba$_{0.75}$Sr$_{0.25}$)Ti$_{1+\delta}$O$_{3+2\delta}$ ceramics with a higher non-stoichiometric level exhibit a weaker diffuse ferroelectric-paraelectric phase transition, which is in accordance with the previous conclusion drawn from the discussion of ΔT_m. It is found that the smaller grain size is beneficial to obtaining a more broadened Curie peak in the BST ceramics due to the grain-boundary effect.[24] The average grain size of the (Ba$_{0.75}$Sr$_{0.25}$)Ti$_{1+\delta}$O$_{3+2\delta}$ samples increases with the increasing δ value, as mentioned previously. Therefore, the diffuse phase transition for high δ samples is weaker than that for low δ ones.

Figure 3 also provides the dielectric response of the (Ba$_{0.75}$Sr$_{0.25}$)Ti$_{1+\delta}$O$_{3+2\delta}$ ceramics at various frequencies. The relative dielectric constant (in the $T<T_m$ range) decreases with the increase of the test frequency. The ε_m and T_m of the (Ba$_{0.75}$Sr$_{0.25}$)Ti$_{1+\delta}$O$_{3+2\delta}$ ceramics at 1 kHz, 10 kHz, 100 kHz and 500 kHz are shown in **Table 4**. The T_m for the R1, R2, R3, and R4 samples shifts only 1 °C towards higher temperature with increasing frequency. For the R0 sample, there is no shift in T_m at all. The ε_m for all the (Ba$_{0.75}$Sr$_{0.25}$)Ti$_{1+\delta}$O$_{3+2\delta}$ ceramics shows an obvious frequency dispersion.

Table 4: ε_m and T_m for (Ba$_{0.75}$Sr$_{0.25}$)Ti$_{1+\delta}$O$_{3+2\delta}$ ceramics at different frequencies

Sample No.	δ	ε_m				T_m (°C)			
		1 kHz	10 kHz	100 kHz	500 kHz	1 kHz	10 kHz	100 kHz	500 kHz
R0	0	6565	6494	6414	6383	−1	−1	−1	−1
R1	0.005	8123	8021	7901	7912	7	8	8	8
R2	0.01	8330	8215	8077	7964	6	7	7	7
R3	0.015	7842	7695	7528	7396	8	8	9	9
R4	0.02	9742	9469	9152	8870	12	12	12	13

4 CONCLUSIONS

Ti-rich (Ba$_{0.75}$Sr$_{0.25}$)Ti$_{1+\delta}$O$_{3+2\delta}$ ceramics for low-frequency capacitor applications were prepared by a conventional solid-state method. The microstructures, dielectric properties and ferroelectric-paraelectric phase transition were investigated with a non-stoichiometric level by SEM, XRD and an LCR measuring system. The following was observed:

1) All the (Ba$_{0.75}$Sr$_{0.25}$)Ti$_{1+\delta}$O$_{3+2\delta}$ ceramics ($\delta = 0.005$, 0.01, 0.015, 0.02) are single-phase solid solutions with a typical tetragonal perovskite structure.

2) With the increasing δ value, the abnormal grain growth occurs and the average grain size of the (Ba$_{0.75}$Sr$_{0.25}$)Ti$_{1+\delta}$O$_{3+2\delta}$ ceramics increases.

3) The enhanced spontaneous polarization takes the main responsibility for the increase of the transition

Figure 5: Plots of $\ln(1/\varepsilon_r - 1/\varepsilon_m)$ as a function of $\ln(T-T_m)$ for (Ba$_{0.75}$Sr$_{0.25}$)Ti$_{1+\delta}$O$_{3+2\delta}$ ceramics (The symbols: experimental data; the solid line: fitting plot)

Legend:
- R0 $\gamma = 1.47026$
- R1 $\gamma = 1.45685$
- R2 $\gamma = 1.46651$
- R3 $\gamma = 1.30255$
- R4 $\gamma = 1.03711$

temperature T_m as well as the increase of the dielectric constant ε_{rRT} and ε_m when δ increases.

4) The low-temperature ($T \leq T_m$) frequency dispersion of the relative dielectric constant can be found and the diffuse phase-transition behavior is suppressed with an increasing δ value in the (Ba$_{0.75}$Sr$_{0.25}$)Ti$_{1+\delta}$O$_{3+2\delta}$ ceramics.

Acknowledgements

5 REFERENCES

[1] L. Li, M. Wang, D. Guo, R. Fu, Q. Meng, Effect of Gd amphoteric substitution on structure and dielectric properties of BaTiO$_3$-based ceramics, J. Electroceram., 30 (**2013**) 129–132, doi:10.1007/s10832-012-9773-9

[2] M. C. Ferrarelli, C. C. Tan, D. C. Sinclair, Ferroelectric, electrical, and structural properties of Dy and Sc co-doped BaTiO$_3$, J. Mater. Chem., 21 (**2011**) 6292–6299, doi:10.1039/C0JM04429F

[3] T. Badapanda, V. Senthil, S. Panigrahi, S. Anwar, Diffuse phase transition behavior of dysprosium doped barium titanate ceramic, J. Electroceram., 31 (**2013**) 55–60, doi:10.1007/s10832-013-9808-x

[4] D. Y. Lu, S. Z. Cui, Defects characterization of Dy-doped BaTiO$_3$ ceramics via electron paramagnetic resonance, J. Eur. Ceram. Soc., 34 (**2014**) 2217–2227, doi:10.1016/j.jeurceramsoc.2014.02.003

[5] D. Y. Lu, L. Zhang, X. Y. Sun, Defect chemistry of a high-k žY5V' (Ba$_{0.95}$Eu$_{0.05}$)TiO$_3$ ceramic, Ceramics International, 39 (**2013**) 6369–6377, doi:10.1016/j.ceramint.2013.01.063

[6] X. G. Tang, K. H. Chew, H. L. W. Chan, Diffuse phase transition and dielectric tunability of Ba(Zr$_y$Ti$_{1-y}$)O$_3$ relaxor ferroelectric ceramics, Acta Mater., 52 (**2004**) 5177–5183, doi:10.1016/j.actamat.2004.07.028

[7] X. P. Jiang, M. Zeng, H. L. W. Chan, C. L. Choy, Relaxor behaviors and tunability in BaZr$_{(0.35)}$Ti$_{(0.65)}$O$_3$ ceramics, Mater. Sci. Eng. A, 438–440 (**2006**) 198–201, doi:10.1016/j.msea.2006.02.109

[8] J. H. Jeon, Y. D. Hahn, H. D. Kim, Microstructure and dielectric properties of barium–strontium titanate with a functionally graded structure, J. Eur. Ceram. Soc., 21 (**2001**) 1653–1656, doi:10.1016/S0955-2219(01)00085-1

[9] B. Su, T. W. Button, Microstructure and dielectric properties of Mg-doped barium strontium titanate ceramics, J. Appl. Phys., 95 (**2004**), 1382–1385, doi:10.1063/1.1636263

[10] Z. Li, H. Fan, J. Wang, S. Jia, Diffusion phase transition and aging properties induced by B-site disorder in Na-doped barium strontium titanium ceramics, J. Mater. Sci., Mater. Electron., 25 (**2014**) 5581–5592, doi:10.1007/s10854-014-2347-7

[11] S. Dupuis, S. Sulekar, J .H. Kim, H. Han, P. Dufour, C. Tenailleau, J. C. Nino, S. Guillemet-Fritsch, Colossal permittivity and low losses in Ba$_{1-x}$Sr$_x$TiO$_{3-\delta}$ reduced nanoceramics, J. Eur. Ceram. Soc., 36 (**2016**) 567–575, doi:10.1016/j.jeurceramsoc.2015.10.017

[12] B. Su, J. E. Holmes, B. L. Cheng, T. W. Button, Processing effects on the microstructure and dielectric properties of barium strontium titanate (BST) ceramics, J. Electroceram., 9 (**2002**) 111–116, doi:10.1023/A:1022850205284

[13] J. Zhang, J. Zhai, X. Chou, X. Yao, Influence of rare-earth addition on microstructure and dielectric behavior of Ba$_{0.6}$Sr$_{0.4}$TiO$_3$ ceramics, Mater. Chem. Phys., 111 (**2008**) 409–413, doi:10.1016/j.matchemphys.2008.04.050

[14] C. Zhao, X. Y. Huang, H. Guan, C. H. Gao, Effect of Y$_2$O$_3$ and Dy$_2$O$_3$ on dielectric properties of Ba$_{0.7}$Sr$_{0.3}$TiO$_3$ series capacitor ceramics, J. Rare Earth, 25 (**2007**)197–200, doi:10.1016/S1002-0721(07)60468-2

[15] Y. Li, Y. Qu, Dielectric properties and substitution mechanism of samarium-doped Ba$_{0.68}$Sr$_{0.32}$TiO$_3$ ceramics, Mater. Res. Bull., 44 (**2009**) 82–85, doi:10.1016/j.materresbull.2008.03.030

[16] C. Zhang, Z. Ling, F. Chen, G. Jian, Y. Li, The dielectric properties and phase transition of Ho$_2$O$_3$ modified barium strontium titanate ceramics for capacitor applications, J. Mater. Sci.: Mater. Electron., 29 (**2018**) 331–335, doi:10.1007/s10854-017-7920-4

[17] U. Syamaprasad, R. K. Galgali, B. C. Mohanty, Capacitor ceramics in pure and doped Ba$_{0.71}$Sr$_{0.29}$TiO$_3$, Mater. Lett., 8 (**1989**) 36–40, doi:10.1016/0167-577X(89)90092-X

[18] C. Zhang, F. Chen, Z. Ling, X. Zhong, G. Jian, Y. Li, The dielectric properties and diffuse phase transition of non-stoichiometric barium strontium titanate based capacitor ceramics, J. Mater. Sci.: Mater. Electron., 29 (**2018**) 9397–9405, doi:10.1007/s10854-018-8972-9

[19] H. Dong, D. Jin, C. Xie, J. Cheng, L. Zhou, J. Chen, Compositionally inhomogeneous Ti-excess barium strontium titanate ceramics with a robust dielectric temperature stability, Mater. Lett., 135 (**2014**) 83–86, doi:10.1016/j.matlet.2014.07.127

[20] S. Yun, X. Wang, B. Li, D. Xu, Dielectric properties Ca-substituted barium strontium titanate ferroelectric ceramics, Solid State Commun., 143 (**2007**) 461–465, doi:10.1016/j.ssc.2007.06.031

[21] C. Zhang, Z. Ling, G. Jian, F. Chen, Dielectric properties and point defect behavior of antimony oxide doped Ti deficient barium strontium titanate ceramics, Trans. Nonferr. Met. Soc. China, 27 (**2017**) 2656–2662, doi:10.1016/S1003-6326(17)60294-2

[22] J. Zhai, X. Yao, J. Shen, L. Zhang, H. Chen, Structural and dielectric properties of Ba(Zr$_x$Ti$_{1-x}$)O$_3$ thin films prepared by the sol-gel process, J. Phys. D: Appl. Phys., 37 (**2004**) 748–752, doi:10.1088/0022-3727/37/5/016

[23] C. Zhang, F. Chen, Z. Ling, G. Jian, Y. Li, Microstructure and dielectric properties of La$_2$O$_3$ doped Ti-rich barium strontium titanate ceramics for capacitor applications, Mater. Sci.-Poland, 35 (**2018**) 806–815, doi:10.1515/msp-2017-0105

[24] C. Zhang, Z. Ling, G. Jian, The defect chemistry and dielectric properties of Sb$_2$O$_3$ doped nonstoichiometric barium strontium titanate ceramics, J. Mater. Sci.: Mater. Electron., 27 (**2016**) 11770–11776, doi:10.1007/s10854-016-5316-5